Organic &
Biomolecular
Chemistry

Cite this: *Org. Biomol. Chem.*, 2011, **9**, 4811

www.rsc.org/obc

PAPER

Studies on [3]pseudorotaxane formation from a bis-azacrown derivative as host and imidazolium ion-derivatives as guest†

Amal Kumar Mandal, Moorthy Suresh and Amitava Das*

Received 2nd December 2010, Accepted 1st March 2011
DOI: 10.1039/c0ob01106a

A new host molecule, having two azacrown derivatives bridged by luminescent naphthalene diimide functionality, is found to form a [3]pseudorotaxane derivative with imidazolim ion-based guest molecules in non-polar solvents through hydrogen-bonded adduct formation. Depending upon the length of the covalent linker that links the imidazolium ion and the luminescent naphthalene fragment in the guests, the [3]pseudorotaxane adducts adopt different conformation or orientation with varying π–π/donor–acceptor interaction. The mechanism for the naphthalene-based luminescence quenching by NDI fragment on adduct formation was found to be a combination of static, as well as dynamic with static quenching as the dominant one.

Studies on the influences that different structural parameters and nonbonding interactions play in achieving a supramolecular assembly comprises one of the most fascinating areas of contemporary research.[1] The consequence of such studies has more significance when it is possible to probe the effect of the variation(s) in structure of the host or guest fragment in adopting or stabilizing a specific conformation in the host–guest noncovalent complex.[2c] Such studies using tailor-made host and guest molecules with predicted spatial orientation or topology are key in developing a deeper insight into understanding more complicated supramolecular structures where individual molecular components are held by various non-bonded interactions.[2] The importance of such noncovalent interactions in supramolecular assemblies in biological systems and bioinspired material is also well documented. Any change in molecular conformation or orientation of the individual component in such an assembly is known to influence greatly the activity or property of such a noncovalent complex.[3] Thus, orientation–activity correlation in designed supramolecular assemblies is expected to help in understanding the change in activity pattern of bioactive fragments like peptides, proteins *etc.* with conformational change(s) in various natural/biological assemblies; where relative stability of different conformations is the manifestation of the change(s) in any or a combination of these non-bonded interactions.[4] For such purpose-build supramolecular assemblies, the design aspect involves various non-covalent interactions, like ion–dipole interaction,[5] hydrogen bonding,[6] π-stacking,[7] and charge transfer interaction.[8] More importantly, appropriate derivatization of the host and guest fragments with a judiciously chosen photoactive donor or acceptor fragment allows the desired handle to probe the supramolecular complex formation. However, such examples are not very common in the literature.[9,10] Recently Rebek *et al.* have shown that intermolecular resonance energy transfer (RET) between pyrene and perylene moieties occur when monofunctionalized pyragallol or resorcinol arene moieties form self assembled hexameric capsule like architecture. It has been shown that the formation of such self-assembled structures is a random process and one out of many conformers and assemblies could show the RET process.[9a,9b] In one of our recent reports we have demonstrated that for a donor–acceptor assembly, the resonance energy transfer process and thereby the new optical response can further be used to probe the folding–unfolding movement in a definite self-assembled system; where π-stacking interaction plays an important role.[10] Iverson has shown that a π-stacking interaction can be utilized in achieving a folded conformation in solution for a certain aedamer,[11] where the efficiency of the π-stacking interactions and the consequential optical responses are dependent on the length and flexibility of the spacer linking the two aromatic fragments involved in the π-stacking interaction. Wilson *et al.* recently identified the specific π-stacking pair among the nine combination of donors and acceptors grafted on a macromolecular backbone. More importantly, they have shown that the efficiency of the π-stacked assembly could be probed based on the studies of static and dynamic quenching.[8b]

We could demonstrate through static and dynamic quenching studies that the π-stacking interaction efficiency and thus the donor (naphthalene)–acceptor (NDI) is dependant on the spacer that links the imidizolium ion and the naphthalene unit in the guest moiety. The acceptor property of the NDI-fragment was ascertained from its relatively lower reduction potential as compared to the naphthalene moiety.[13,11b] The complex formation, *i.e.*, the [3]pseudorotaxane formation between **H** and $\mathbf{G_1}$ or $\mathbf{G_2}$

Central Salt & Marine Chemicals Research Institute (CSIR), Bhavnagar: 364002, Gujarat, India. E-mail: amitava@csmcri.org; Fax: +91 278 2567562; Tel: +91 278 2567760 [672]

† Electronic supplementary information (ESI) available: ^{1}H NMR, ^{13}C NMR, and ESI-MS characterization. See DOI: 10.1039/c0ob01106a

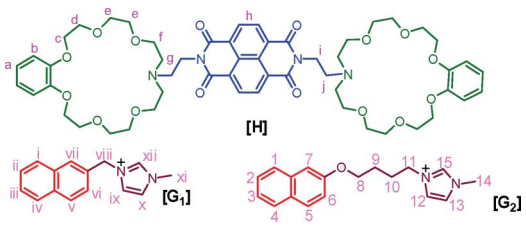

Fig. 1 Structures of host and guest components.

(Fig. 1), was characterised by ^{1}H-NMR, ESI-Ms, electronic and fluorescence spectroscopic studies.

The methodology that was adopted for the synthesis of the azacrown derivative (**H**) is shown in Scheme 1. Alkylation of 1,2-dihydroxy benzene was achieved with reasonable yield by reaction with 2-[2-(2-chloroethoxy)-ethoxy]-ethanol in a suspension of K_2CO_3 in DMF (dry) as solvent.

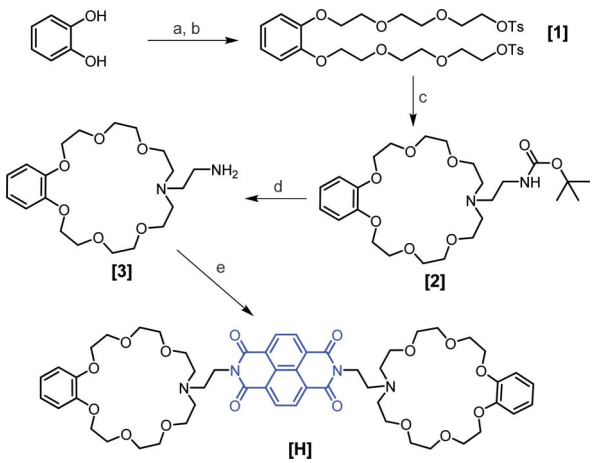

Scheme 1 Synthesis of **H**. Reagents and conditions: (a) $Cl(CH_2O)_3H$, K_2CO_3, KI, DMF, 90 °C (b) TsCl, NaOH, THF/H_2O, 0 °C - RT. (c) K_2CO_3, KI, $H_2N(CH_2)_2NHBoc$, CH_3CN, 81 °C. (d) HCl, Et_2O-DCM, RT. (e) 1,4,5,8-Naphthalene dianhydride, CH_3CN, 81 °C

Chromatographic purification yielded the bis hydroxy intermediate (yield: 53.3%), which was further converted to the corresponding bis tosylate derivative (**1**; yield: 78%). The intermediate product (**1**) was allowed to react with N-Boc-ethyldiamine to give the desired compound **2**.[14] Purification of **2** was achieved by gravity chromatography and the pure protected form of the aza-macrocycle was isolated in 57.64% yield. Finally deprotection of the N-Boc-derivative resulted in the desired amine derivative **3**, which on treatment with 1,4,5,8-naphthalenedianhydride in acetonitrile afforded the final product **H** in 40% yield after the necessary purification by column chromatography.

The preparation of imidazolium cationic salts $\mathbf{G_1}$ and $\mathbf{G_2}$ was done mainly in two steps. The reaction of the 1-methylimidazole with the respective bromoalkyl derivative (2-bromomethyl naphthalene for $\mathbf{G_1}$ and 2-(4-bromobutoxy)naphthalene for $\mathbf{G_2}$) in toluene resulted in the bromide salt of $\mathbf{G_1}$ and $\mathbf{G_2}$; while the desired and corresponding PF_6^- salt was isolated by anion exchange in aqueous medium.

All compounds have been characterised by elemental analysis and various spectroscopic methods like, ^{1}H-NMR, ^{13}C-NMR and ESI-MS. Analytical and spectroscopic data matched well to ascertain the structure proposed for the respective intermediate and final host (**H**)/guest (**G**) compounds, as well as the desired purity.

As mentioned earlier, 1,3-disubstituted imidazolium salts are known to form an inclusion complex with DB24C8 or its derivatives through intermolecular hydrogen-bond formation as demonstrated by different research groups.[12] In 1,3-disubstituted imidazolium salts, all protons on the imidazolium ring are quite acidic, as the positive charge is delocalized over the entire imidazolium ring. The acidic hydrogen atoms participate in hydrogen-bond formation with the lone pair of electrons of the oxygen/nitrogen atoms on the azacrown moiety and this accounts for the stability of the adduct formed. A mass spectrometry study confirmed the formation of such a hydrogen bonded complex. Electrospray ionisation mass spectroscopy (ESI-Ms) is used to "fish" loosely bonded supramolecular complexes, obtained by mixing one equivalent of the host molecule (**H**) with 2.5 mole equivalent of the respective guest molecule ($\mathbf{G_1}$ or $\mathbf{G_2}$) in CH_2Cl_2 solution. The ESI-mass spectra in the positive ion mode showed *m/z* peaks at 1785.11 and 1735.80, respectively for use of $\mathbf{G_1}$ and $\mathbf{G_2}$ as the guest fragment. *m/z* peaks at 1785.11 corresponds to [$\mathbf{H.2G_1}$ + Na^+] and thus confirms the formation of a 1 : 2 complex between **H** and $\mathbf{G_1}$; while for *m/z* peaks at 1735.80 correspond to a similar 1 : 2 complexation and confirmed formation of the adduct [$\mathbf{H.2G_2}$ – PF_6^-]$^+$.

The complexation of **H** with $\mathbf{G_1}$ or $\mathbf{G_2}$ was studied in detail by ^{1}H-NMR spectra in CD_2Cl_2 at 25 °C. Hydrogen bonded adduct formation between **H** and $\mathbf{G_1}$ or $\mathbf{G_2}$ is expected to be more efficient in a relatively less polar solvent. For solvents with higher polarity, the efficient solvation of the cationic imidizolium ion could compete with the H-bonded adduct formation between the cationic guest ($\mathbf{G_1}$ or $\mathbf{G_2}$) and the azacrown ether-based host molecule. Experimental studies also revealed that the host (**H**) and guest component ($\mathbf{G_1}$ or $\mathbf{G_2}$) in the hydrogen-bonded adduct $\mathbf{H.2G_1}$ or $\mathbf{H.2G_2}$ dethreads in the presence of polar solvents like methanol or CD_3OD. We recorded ^{1}H-NMR spectra for **H** in the absence and the presence of $\mathbf{G_1}$ (Fig. 2A) and $\mathbf{G_2}$ (Fig. 2B) in CD_2Cl_2.

Previous reports on inclusion complex formation between crown ether derivatives and imidizolium ion suggest three possible modes of interaction. The most prominent one is the hydrogen bonding interaction between O_{Crown} and acidic C–H proton of imidazolium ion ($\{C–H\}_{Imidazolium}$) for [$\{C–H\}_{Imidazolium} \cdots O_{Crown}$]-interaction. π–π stacking interactions between the electron poor imidazolium ring and aryl groups of the crown ether-based host is the second one which is expected to contribute to the stability of the adduct formation. The possibility of such an interaction for an analogous system was reported earlier.[12a,d] Apart from H-bonding and π–π stacking interactions, induced dipole–dipole interaction between imidizolium ion and O_{Crown} having –δ charge could also contribute to the overall stability of the adduct formation; such a proposition was made independently by Schmitzer *et al.* and Pursiainen *et al.*[12a,d,15] However, this induced dipole–dipole interaction is expected to be weaker as compared to two previous modes of interaction discussed. All these reports have unambiguously shown that an interwoven complex formation takes place between the crown ether-based host molecule and imidizolium ion derivative(s) as guest through detailed ^{1}H-NMR studies.

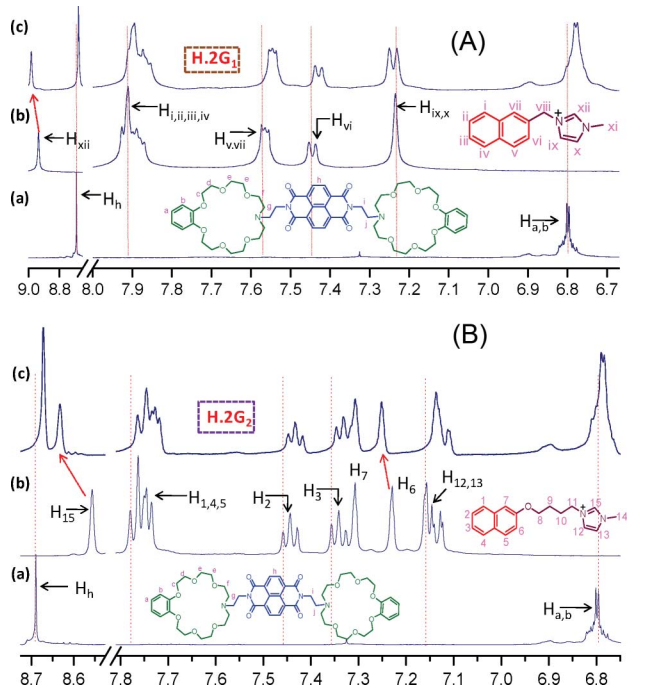

Fig. 2 (A) Partial ^{1}H-NMR spectra recorded in CD_2Cl_2 at 25 °C of (a) 5.43 mM **H**; (b) in presence of 10.89 mM $\mathbf{G_1}$ and (c) in the presence of 10.89 mM of $\mathbf{G_1}$ and 5.43 mM **H**. (B) Partial ^{1}H-NMR spectra recorded in CD_2Cl_2 at 25 °C of (a) 4.68 mM **H**; (b) in presence of 9.38 mM $\mathbf{G_2}$ and (c) in the presence of 9.38 mM $\mathbf{G_2}$ and 4.68 mM **H**.

The nature of the shifts in the ^{1}H-NMR spectra for the two major modes of interaction, namely H-bonding and π–π stacking interactions are expected to be quite different. One would expect a down field shift for hydrogen atom(s) involved in H-bonding interaction(s). For π–π stacking/arene donor–acceptor interactions, upfield or down field shifts for hydrogen atoms of aromatic/arene moiety(ies) could be observed depending upon the nature and degree of shielding influence(s) that it experience(s) due to its specific orientation with respect to the other interacting π-system.[11]

In the present study, we have recorded the ^{1}H-NMR spectra for host molecule (**H**) in the absence and presence of two mole equivalent of the respective guest molecule ($\mathbf{G_1}$ or $\mathbf{G_2}$) (Fig. 2A and 2B) – a condition that allows formation of the 1 : 2 adduct between **H** and $\mathbf{G_1}$ or $\mathbf{G_2}$, *i.e.*, $\mathbf{H.2G_1}$ or $\mathbf{H.2G_2}$ and this was evident from the mass spectral results.†

A comparison of the ^{1}H-NMR spectra for $\mathbf{H.2G_1}$ (Fig. 2A) with those of free **H** and $\mathbf{G_1}$ fragments revealed that the signals for hydrogen atoms of the arene units of the crown ether moiety were upfield shifted; while those for three imidazolium ion (H_{ix}, H_x and H_{xii}) were downfield shifted. Though small, distinct upfield shifts for the naphthalene protons were observed on adduct formation.

Downfield shifts for the imidazolium ion supports adduct formation ($\mathbf{H.2G_1}$) through H-bond formation involving the [{C–H}$_{\text{Imidazolium}}$ ··· O/N$_{\text{Crown}}$]-interaction. Upfield shifts for the protons of the naphthyl moiety of $\mathbf{G_1}$ and two phenyl rings of **H**, suggests a π–π interaction; observed δ_H for **H** was 8.689 ppm; while that in the hydrogen bonded adduct (*i.e.* for $\mathbf{H.2G_1}$) was 8.679 ppm. However, this upfield shift for the protons of the NDI unit is not very significant and this suggests a weak π–π stacking interaction.

In the case of using $\mathbf{G_2}$ as the guest fragment the pattern of shifts for the individual hydrogen atoms of the **H** and $\mathbf{G_2}$ fragments on adduct formation ($\mathbf{H.2G_2}$) was much different. An appreciable downfield shift for the signal of H_{15} was observed; while little upfield shift for other imidazolium protons (H_{12}, H_{13}) was observed. This presumably suggests a orientation for the imadazolium ring that allows a relatively stronger H-bonding for H_{15} as compared to H_{12} and H_{13}, as well as a weak π–π interaction involving H_{12} and H_{13} and the phenyl ring of **H**. Thus two opposing influences operational for H_{12} and H_{13}, namely H-bonding and π–π interaction, are perhaps responsible for small but distinct upfield shifts for these two protons. For NDI hydrogen atoms (H_h), as well as other protons (barring H_6) of the two naphthalene moieties of $\mathbf{G_2}$, distinct upfield shifts were observed. These suggest a π–π stacking interaction involving an NDI fragment and $\mathbf{G}_{\text{Naphthalene}}$ moieties. Little downfield shift for H_6 suggests that it oriented in the deshielding zone of the NDI fragment. Such an observation is reported by Iverson *et al.* based on ^{1}H NMR, as well as detailed electrostatic surface potential studies.[11a,c] Based on the differences in the observed chemicals shifts for the two adducts, $\mathbf{H.2G_1}$ and $\mathbf{H.2G_2}$, and the associated modes of interaction, two different interaction schemes may be proposed and schematic representation of such interactions are shown in Fig. 3 and 4, respectively. In both cases, *i.e.* for $\mathbf{H.2G_1}$ and $\mathbf{H.2G_2}$, down field shifts for -N–CH_3 protons of the imidazolium unit (H_{xi} for $\mathbf{G_1}$ and H_{14} for $\mathbf{G_2}$) were observed, when compared with free guest molecules.†

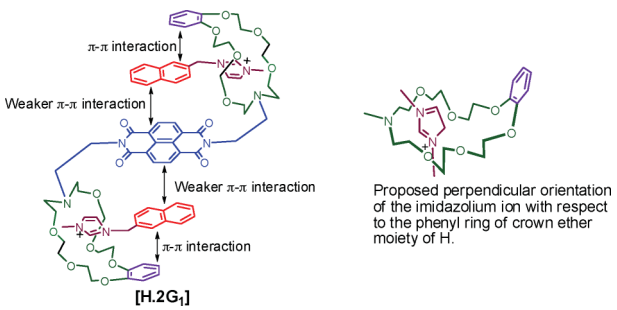

Fig. 3 Schematic presentation of the probable orientation of the **H** and $\mathbf{G_1}$ in the [3]pseudorotaxane $\mathbf{H.2G_1}$ in CH_2Cl_2.

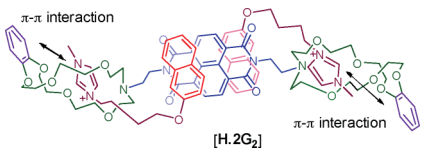

Fig. 4 Schematic presentation of the probable orientation of the **H** and $\mathbf{G_2}$ in the [3]pseudorotaxane $\mathbf{H.2G_2}$ in CH_2Cl_2.

However, it is worth mentioning here that the extent of shifts for the π–π interactions are much smaller than those are usually observed for strongly interacting π–π donor–acceptor systems in highly polar solvents.[8b,c,9] This is understandable as the present study was carried out in a weakly polar solvent medium like CH_2Cl_2 to favour the interwoven complex formation. Further support for the weaker π–π stacking interaction came from the results of the 2D-NOESY spectra for $\mathbf{H.2G_1}$ and $\mathbf{H.2G_2}$.† For $\mathbf{H.2G_2}$ cross peaks were observed for imidazolium protons ($H_{12,13,15}$) and

crown ether protons (H_c, H_f). Analogously, for **H.2G$_1$** cross peaks were observed for imidazolium protons ($H_{IX, X, XII}$) and crown ether protons (H_c, H_f). These confirm the hydrogen bond interaction through space coupling. However, no cross peaks were observed between naphthalene and naphthalenediimide which indicates that these two units are too far away (>5 Å) for any significant π–π stacking interaction. This result also supports our results on steady-state absorption spectral data where no charge transfer band was observed.

Thus, the above results revealed that two different linkers that bind the imidazolium ring to the naphthyl moiety in **G$_1$** and **G$_2$** play an important role in the binding process and thus the relative conformation adopted by the two guests in the respective adducts, *i.e.* **H.2G$_1$** and **H.2G$_2$**, respectively. More importantly, ^{1}H NMR studies revealed an apparent perpendicular orientation of the imidazolium moiety of **G$_1$** in the azacrown cavity of **H.2G$_1$**; while this seemed to be different for **G$_2$** in **H.2G$_2$**. The possibility of such an orientation for the imidizolium ion is confirmed by Rissianen and Pursiainen for analogous inclusion complex formation between imidazolium ion and dibenzo 18-crown-6.[12a]

The absorption and fluorescence spectra of **G$_1$** and **G$_2$** were recorded in CH_2Cl_2 at room temperature. The absorption spectrum of **G$_1$** is dominated by the characteristic absorption band of the naphthalene moiety at 276 nm and a more intense band at shorter wavelength. On excitation at 276 nm, an emission band appeared at 336 nm. For **G$_2$**, absorption and emission bands appeared at 273 and 348 nm, respectively.

A strong absorption band for **H** was observed at 380 nm along with a weaker band at 360 nm. The absorption band at 380 nm was attributed to the S_0–S_1 and/or S_0–S_2 transition associated with the NDI unit. The absorption and emission characteristics of the three molecules are shown in Table 1 and normalized spectra for these units are shown in Fig. 5. Electronic spectra for **H** and **H** in the presence of varying **G$_x$** (x = 1 or 2) were recorded. Even in the presence of 2.25 mole equivalent of **G$_x$** in CH_2Cl_2 (a condition where **H.2G$_x$** adducts exist predominantly), neither any shift of the respective absorption band of the individual component, nor any new absorption band was observed. This nullifies the possibility of the formation of any donor–acceptor type charge transfer complex between acceptor NDI-based host and donor naphthalene-based guest fragments. This agrees well with the results of the ^{1}H-NMR spectra, which predicted a weaker π–π interaction between the two chromophores.

Steady state fluorescence spectra recorded for **G$_1$** or **G$_2$** with increasing [**H**] revealed a steady decrease of emission intensity of the respective molecules (Fig 6). The quenching ratio I_0/I, (where I_0 and I are the emission intensity in the absence and in the presence of **H** respectively) for respective guest molecules (**G$_1$** or **G$_2$**) were plotted against [**H**]. The values for I_0/I with varying [**H**] were plotted using the standard Stern–Volmer relationship, which is shown in expression 1.

Table 1 Absorption and fluorescence spectral details observed for **H**, **G$_1$** and **G$_2$** in CH_2Cl_2 at 25 °C

	Electronic spectral parameters		Fluorescence spectral parameters	
	λ_{max}	ε_{max}/dm^3 mol^{-1} cm^{-1}	λ_{max}	τ/ns
H	380	16352	412	5.37
G$_1$	276	5938	336	10.43
G$_2$	273	3747	348	5.11

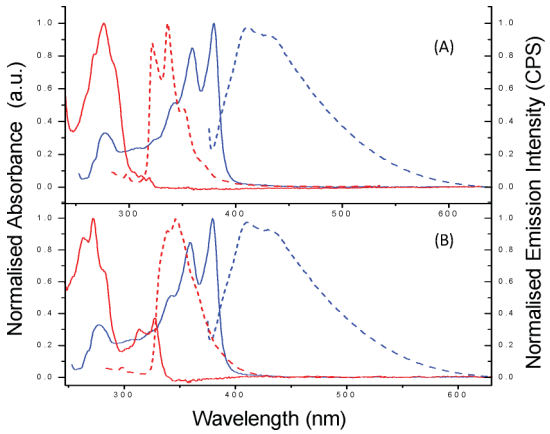

Fig. 5 (a) Absorption (solid line) and fluorescence (dashed line) spectra of **G$_1$** (red) and **H** (blue); (b) Absorption (solid line) and fluorescence (dashed line) spectra of **G$_2$** (red) and **H** (blue) in CH_2Cl_2 at 25 °C.

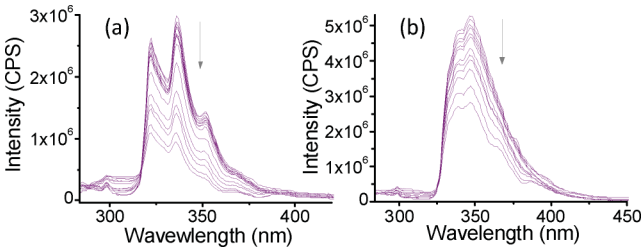

Fig. 6 Luminescence quenching of (a) **G$_1$** (6.76 ×10^{-6} M) and (b) **G$_2$** (6.96 × 10^{-6} M) observed with increasing [**H**]. The arrow highlights the effect of increasing concentration of **H**.

$$\frac{I_0}{I} = 1 + \left(\frac{k_q}{K_e + k_d}\right)[C_Q] = 1 + K_D[C_Q] \quad (1)$$

Where K_q, K_e and K_d are the rate of quenching, emission and deactivation respectively. K_D is the Stern–Volmer quenching constant for collisional deactivation and C_Q is the concentration of quencher. Plots of I_0/I against varying quencher (**H**) concentration were not linear.† An independent plot of I_0/I for **G$_1$** and **G$_2$**, respectively, against increasing [**H**] showed an upward curvature. This tends to suggest that both static and dynamic quenching were operational at the same time. The occurrence of dynamic quenching can also be recognised by measurement of the fluorescence life time of **G$_1$** and **G$_2$** with increasing concentration of **H**.[16a]

The values of static quenching constants for the two respective systems were determined from the initial linear segment of the Stern–Volmer plot for the lowest concentration of the quencher (**H**) and are shown in Table 2. The contribution to quenching through a dynamic (collisional) mechanism was determined from the plot of τ_0^x/τ^x (where τ_0^x and τ^x are the life time of **G$_x$** (x is 1 or 2) in the absence and presence of **H**, respectively) against [**H**] (Fig. 7) and quenching constants for the respective guest molecules were evaluated and are shown in Table 2.

Table 2 Static and dynamic quenching constant values for **H.2G$_1$** and **H.2G$_2$**, along with the formation constant of the ground state host–guest complexes

Static quenching process			Dynamic quenching process		Formation constant
	Static quenching constant/M^{-1}	R^2	Dynamic quenching constant/M^{-1}	R^2	K_f/M^{-1}
H.2G$_1$	2.3×10^4	0.99	1.97×10^2	0.95	1.07×10^4
H.2G$_2$	6.81×10^4	0.99	3.56×10^3	0.93	1.09×10^5

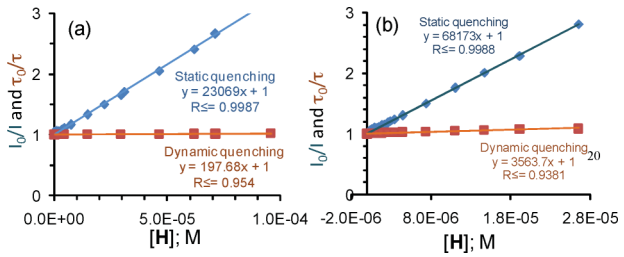

Fig. 7 Linear trend of Stern–Volmer plot for both emission quenching and fluorescence lifetime decrease for (a) **H.2G$_1$** system and (b) **H.2G$_2$** system at low concentration of **H** addition.

Similar procedure was adopted by many researchers for evaluation of the static and dynamic quenching constants and are well documented in the literature.[8b,16]

The formation constant (K_f) for the hydrogen bonded adduct (**H.2G$_1$** and **H.2G$_2$**) was determined from the systematic fluorescence titration[17] and the values for respective complexes are also shown in Table 2. Comparison of the K_f values for **H.2G$_1$** and **H.2G$_2$** suggest that one of the two imidazolium-ion based guests (**G$_2$**), forms a more stable inclusion complex with the same host molecule, **H**. This certainly reflects the higher flexibility of the linker in **G$_2$** as the favorable factor for aligning the donor in a more symmetric fashion for more effective π–π stacking. However, one cannot completely ignore the influence of the different electronic nature of the two different donor units towards the observed difference in binding constants.[8b,c,11a]

To verify the formation of a ground state hydrogen bonded complex, quenching experiments were performed at different excitation wavelengths for both **H.2G$_1$** and **H.2G$_2$** systems (Fig. 8). The data are summarised in Table 3. The value of the static quenching constant appears to decrease with increasing excitation wavelength. This decrease is small but regular for both the **H.2G$_1$** and **H.2G$_2$** systems. This strongly suggests the formation of a ground state complex. The reason for no discernable change of

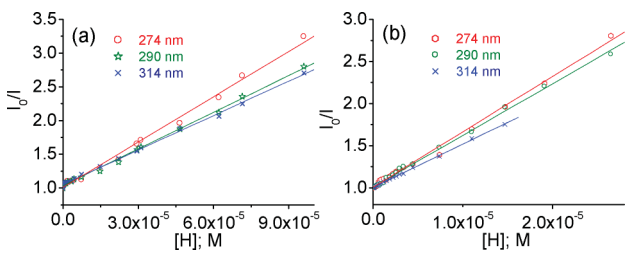

Fig. 8 Linear trend of Stern–Volmer Plot of I_0/I against concentration of **H** at different excitation wavelength (a) for **H.2G$_1$** system (b) for **H.2G$_2$** system.

Table 3 Values of static quenching constants for different excitation wavelengths for **H.2G$_1$** and **H.2G$_2$**

	λ (nm)	Static quenching constants	R^2
H.2G$_1$	274	2.3×10^4	0.99
	290	1.86×10^4	0.97
	314	1.79×10^4	0.99
H.2G$_2$	274	6.81×10^4	0.99
	290	6.27×10^4	0.98
	314	5.1×10^4	0.97

the absorption spectra in the presence and absence of quencher may therefore be due to very similar extinction coefficients (ε) of the fluorophore and fluorophore-quencher complex.[18]

Conclusions

Two imidazolium ion-based molecules (**G$_1$** and **G$_2$**), with different lengths of covalent linker that links the imidazolium unit to the fluorescence active naphthalene moiety, have been used for studying the interwoven complex formation. Detailed ^{1}H-NMR spectral studies revealed that hydrogen bonding interactions ([{C–H}$_{Imidazolium}$ ··· O/N$_{Crown}$]), apart from the weaker π–π/arene–arene donor–acceptor interactions resulted in moderately strong (K_f = 1.07×10^4 for **H.2G$_1$**, K_f = 1.09×10^5 for **H.2G$_2$**) inclusion complex formation in less polar solvents like CH_2Cl_2. Results of the electronic and fluorescence spectral studies also suggest the formation of a ground state complex. Quenching of the luminescence of the naphthalene moiety of the guest molecules (**G$_1$** and **G$_2$**) by the NDI moiety of **H** was found to be predominantly static in nature.

Experimental procedures

^{1}H-NMR spectra were recorded either on a Bruker 200 MHz FT NMR (model: Advance-DPX 200) or on a Bruker 500 MHz FT NMR (model: Advance-DPX 500) spectrometer at room temperature (RT, 25 °C). The chemical shift (δ) data and coupling constant (J) values are given in parts per million and Hertz, respectively, throughout this manuscript unless mentioned otherwise. ESI-MS measurements were carried out on a Waters QTof-Micro instrument. UV-Vis spectra were obtained by using either a Shimadzu UV-3101 PC or a Cary 500 Scan UV-Vis-NIR spectrometer. Steady state emission spectra at room-temperature were obtained using a Fluorolog Horiba Jovin Yvon luminescence spectrofluorimeter. Time resolved emission studies were carried out using Time Correlated Single Proton Counting (TCSPC) technique were carried out using Edinburgh Instruments F900.

Materials and methods

Catechol, 2-[2-(2-chloro-ethoxy)-ethoxy]-ethanol, *p*-toluenesulfonyl chloride, di-*tert*-butyl dicarbonate were obtained from Sigma-Aldrich Chem. Co. and were used as received without any further purification. $[NH_4]^+PF_6^-$ was recrystallised from ethanolic solution before use. All solvents were of reagent grade and were procured from S.D. Fine Chemicals (India) and all solvents were dried and distilled prior to use following standard procedures.

Synthesis

A: 1,2-Dihydroxy benzene (3 g, 27.27 mmole) was dissolved in 70 ml of freshly dried DMF in two neck round bottom flask. To this solution K_2CO_3 powder (11.28 g, 81.81 mmole) was added. Then the reaction mixture turned from brown to violet colour, KI (13.58 g, 81.81 mmole) was added. This mixture was allowed to stir for 15 min, and 2-[2-(2-chloro-ethoxy)-ethoxy]-ethanol (9.16 g, 54.54 mmole) was added *via* a syringe at 60 °C. Then the temperature was raised up to 80 °C and allowed to stir for 5 days. The solvent was removed under reduced pressure and extracted three times with $CHCl_3$ and water. Organic layers were combined and dried over anhydrous sodium sulfate. Solvent was removed under reduced pressure to give crude product which was purified on a silica-gel column, using methanol : dichloromethane (2 : 98 v/v) as an eluent with the yield of (**A**) 5.44 g, 53.3%, as a sticky brown semisolid. ^{1}H-NMR (500 MHz, $CDCl_3$, δ (ppm)): 3.58 (4H, t, J = 4.5), 3.66 (4H, t, J = 4.5); 3.74–3.70 (8H, m), 3.86 (4H, t, J = 4.5), 4.15 (4H, t, J = 4), 6.89 (4H, s). Elemental analysis: Calculated for $C_{18}H_{30}O_8$: C 57.74, H 8.08; found: C, 57.50; H, 8.10. (ESI-MS) calcd for $C_{18}H_{30}O_8$: 374.19, found: 397.41 $[M + Na]^+$.

1: Compound [**A**] (5.44 g, 14.56 mmole) was dissolved in THF (40 ml) and 5 ml NaOH solution (10 M) was added to it at 0 °C. *p*-Toluenesulfonyl chloride (9.71 g, 50.96 mmole) in 15 ml of THF was added dropwise over a period of 30 min to the reaction mixture at 0 °C with vigorous stirring. The reaction was stopped after 5 days. The solvent was removed under reduced pressure and extracted three times with $CHCl_3$ and water. The organic layers were combined and dried over anhydrous sodium sulfate. Solvent was removed under reduced pressure to give crude product. This was purified on a silica-gel column, using $CH_3OH : CH_2Cl_2$ (2 : 98 v/v) as an eluent with the yield of (**1**) 7.75 g, 78.0%, as a sticky brown mass. ^{1}H-NMR (500 MHz, $CDCl_3$, δ (ppm)): 2.41 (6H, s), 3.59 (4H, t, J = 4), 3.69–3.63 (8H, m), 3.82 (4H, t, J = 5), 4.13 (4H, t, J = 5), 6.90 (4H, s), 7.31 (4H, d, J = 8), 7.79 (4H, d, J = 8.5). ^{13}C-NMR: 150.7, 147.0, 134.8, 131.8, 129.8, 128.0, 123.4, 116.2, 72.5, 71.5, 70.5, 23.3. Elemental analysis: Calculated for $C_{32}H_{42}O_{12}S_2$: C 56.29, H 6.20; found: C 56.10, H 6.10. (ESI-MS): Calcd. for $C_{32}H_{42}O_{12}S_2$: 682.21, found: 683.40 $[M + 1]^+$.

2: Compound **1** (2.0 g, 2.92 mmole) and N-Boc ethylene diamine (0.468 g, 2.92 mmole) were dissolved in 15 ml of dry acetonitrile. To this solution K_2CO_3 powder (4.04 g, 29.28 mmole) and KI (728 mg, 4.39 mmole) were added. The whole reaction mixture was allowed to reflux for 24 h under complete nitrogen atmosphere. After filtration of the cooled reaction mixture, solvent was removed from the filtrate under reduced pressure and extracted three times with $CHCl_3$ and water. Organic layers were combined and dried over anhydrous sodium sulfate. Solvent was removed under reduced pressure to give crude product. This was purified on a silica-gel column using chloroform : methanol (92 : 8) as an eluent with yield of 0.84 g, 57.6% of the desired product **2**. ^{1}H-NMR (200 MHz, CD_2Cl_2, δ (ppm)): 6.89 (4H, s), 4.11 (4H, s), 3.85 (4H, s), 3.72 (4H, s), 3.63 (4H, s), 3.53 (4H, s), 3.10 (2H, s), 2.72 (4H, s), 2.58 (2H, s), 1.40 (9H, s). ^{13}C-NMR (500 MHz, CD_2Cl_2, δ (ppm)): 155.4, 148.4, 120.8, 113.7, 77.8, 70.3, 69.9, 69.2, 68.4, 68.0, 53.8, 52.7, 38.1, 27.6. Elemental analysis: Calculated for $C_{25}H_{42}N_2O_8$: C 60.22, H 8.49, N 5.62; found: C 60.30, H 8.40, N 5.60. ESI-MS: Calc. for $C_{25}H_{42}N_2O_8$: 498.60, found: 499.56 $[M + 1]^+$.

3: Compound **2** (1.82 g, 3.64 mmole) was dissolved in 20 ml of dichloromethane and then treated with 15 ml of HCl-saturated ether solution. The reaction mixture was stirred for 24 h at room temperature. The solvents were removed under vacuum conditions. The mixture was extracted three times using dichloromethane and water, during extraction the pH of the mixture was adjusted to 12 using NH_4OH. The organic layers were combined and dried over anhydrous sodium sulfate. Solvent was removed under reduced pressure to give crude product. This crude product was loaded on an alumina column and eluted by chloroform : methanol (92 : 8) to give compound **3** as a sticky brown solid with the yield of 1.16 g, 80.0%. ^{1}H-NMR (500 MHz, $CDCl_3$, δ (ppm)): 6.87 (4H, s), 4.10 (4H, t, J = 4), 3.86 (4H, t, J = 4), 3.68 (4H, t, J = 4), 3.61 (4H, t, J = 4), 3.45 (4H, t, J = 4.75), 2.76 (4H, t, J = 4.5), 2.74–2.69 (4H, m). ^{13}C-NMR (500 MHz, $CDCl_3$, δ (ppm)): 149.3, 124.1, 115.3, 72.3, 72.2, 71.5, 70.2, 57.3, 53.2, 40.4. Elemental analysis: Calculated for $C_{20}H_{34}N_2O_6$: C 60.22, H 8.60, N 7.03; found: C 60.10, H 8.50, N 7.00. ESI-MS: Calc. for $C_{20}H_{34}N_2O_6$: 398.49, found: 399.65 $[M + 1]^+$.

H: In a 100 ml two neck round bottom flask, compound **3** (0.489 g, 1.22 mmole) was added to a suspension of 1,8:4,5-naphthalene dianhydride (0.15 g, 0.55 mmole) in 50 ml of acetonitrile. The reaction mixture was refluxed for 3 days. The hot reaction mixture was filtered. All the solvents were evaporated and loaded on an alumina column using chloroform : methanol (98 : 2) as an eluent to yield the final compound **H** with the yield of 0.23 g, 40.0%. ^{1}H-NMR (500 MHz, CD_2Cl_2, δ (ppm)): 8.69 (4H, s), 6.80 (4H, d, J = 10), 6.79 (4H, d, J = 9.5), 4.25 (4H, t, J = 7.25), 4.05 (8H, t, J = 4.75), 3.80 (8H, t, J = 4.5), 3.63–3.62 (12H, m), 3.56–3.54 (16H, m), 2.85 (8H, s). ^{13}C-NMR (500 MHz, $CDCl_3$, δ (ppm)): 162.8, 148.9, 130.8, 126.6, 121.4, 114.5, 70.9, 70.7, 70.1, 69.9, 69.2, 54.3, 52.3. ESI-MS (HRMS): Calculated for $\mathbf{H}H^+$ ($C_{54}H_{69}N_4O_{16}$):1029.47; Experimentally found: 1029.47. mp: 152 °C.

G_1: (0.5 g, 2.26 mmole) of bromomethyl naphthalene and (0.185 g, 2.26 mmole) of 1-methyl imidazole was dissolved in 20 ml of dry toluene and refluxed for 24 h under N_2 atmosphere. Then the reaction mixture was cooled and kept in a freezer overnight. The white sticky solid which was settled in the bottom was separated out and washed several times with toluene to give the bromide salt. finally anion exchange in water using NH_4PF_6 gave the desired PF_6^- salt of G_1 with the yield of 0.50 g, 60.0%. ^{1}H-NMR (500 MHz, CD_2Cl_2, δ (ppm)): 8.94 (1H, s), 7.92–7.87 (4H, m), 7.57–7.55 (2H, d, J = 9), 7.40 (1H, d, J = 8.5), 7.23 (2H, s), 5.49 (2H, s), 3.93 (3H, s). ^{13}C-NMR (200 MHz, CD_3CN, δ (ppm)): 136.3, 133.2, 131.3, 129.1, 128.0, 127.0, 125.6, 124.0, 122.4, 117.4, 52.9, 35.9. Elemental analysis: Calculated for $C_{15}H_{15}N_2PF_6$: C 48.92, H 4.11, N 7.61; found: C 49.00, H 4.10, N 7.50. ESI-MS: Calc. for $C_{15}H_{15}N_2PF_6$: 368.29, found: 223.12 $[M - PF_6^-]^+$. mp: 86 °C.

G_2: (0.4 g, 1.43 mmole) of bromobutyl naphthalene and (0.118 g, 1.43 mmole) of 1-methyl imidazole were dissolved in 20 ml of dry toluene and refluxed for 24 h under N_2 atmosphere. Then the reaction mixture was cooled and kept in a freezer overnight. The white sticky solid which was settled in the bottom was separated out and washed several times with toluene to give the bromide salt. Finally anion exchange in water using NH_4PF_6 gave the desired PF_6^- salt of G_2 with the yield of 0.30 g, 50.0%. ^{1}H-NMR (500 MHz, CD_2Cl_2, δ (ppm)): 8.56 (1H, s), 7.78–7.74 (3H, m), 7.45 (1H, t, J = 7.5), 7.34 (1H, t, J = 7.5), 7.31 (1H, s), 7.23 (1H, s), 7.16 (1H, s),

7.14 (1H, d, J = 9), 4.30 (2H, t, J = 7.5), 4.15 (2H, t, J = 5.75), 3.90 (3H, s), 2.19–2.13 (2H, m), 1.94–1.89 (2H, m). ^{13}C-NMR (200 MHz, CD_3CN, δ (ppm)): 135.9, 129.3, 127.5, 126.5, 123.7, 122.3, 118.7, 117.3, 106.7, 67.0, 49.3, 35.8, 26.7, 25.4. Elemental analysis: Calculated for $C_{18}H_{21}N_2OPF_6$: C 50.71, H 4.96, N 6.57; found: C 50.80, H 5.01, N 6.50. ESI-MS: Calc. for $C_{18}H_{21}N_2OPF_6$: 426.37, found: 281.36 $[M - PF_6^-]^+$. mp: 78 °C.

Acknowledgements

The authors wish to acknowledge DST and CSIR for financial support. A. D thanks P. K. Ghosh for his keen interest in this work. A. K. M and M. S acknowledge CSIR for a research fellowship.

References

1 (*a*) S. Sivakova and S. J. Rowan, *Chem. Soc. Rev.*, 2005, **34**, 9; (*b*) G. Cooke and V. M. Rotello, *Chem. Soc. Rev.*, 2002, **31**, 275; (*c*) J.-M. Lehn, *Supramolecular chemistry: Concepts and Perspectives*, Wiley VCH, Weinheim, 1995; (*d*) O. Takahashi, Y. Kohno and M. Nishio, *Chem. Rev.*, 2010, **110**, 6049–6076; (*e*) C. Zhang, S. Li, J. Zhang, K. Zhu, N. Li and F. Huang, *Org. Lett.*, 2007, **9**, 5553–5556; (*f*) M. Zhang, K. Zhu and F. Huang, *Chem. Commun.*, 2010, **46**, 8131–8141; (*g*) C. Zhang, K. Zhu, S. Li, J. Zhang, F. Wang, M. Liu, N. Li and F. Huang, *Tetrahedron Lett.*, 2008, **49**, 6917–6920.

2 (*a*) C. A. Royer, *Chem. Rev.*, 2006, **106**, 1769–1784; (*b*) S. P. Fletcher, F. Dumur, M. M. Pollard and B. L. Feringa, *Science*, 2005, **310**, 80–82; (*c*) L. Hedstrom, *Chem. Rev.*, 2002, **102**, 4501–4524; (*d*) J. Wang and M. A. El-Sayed, *Biophys. J.*, 2000, **78**, 2031; (*e*) W. A. Loughlin, J. D. A. Tyndall, M. P. Glenn and D. P. Fairlie, *Chem. Rev.*, 2004, **104**, 6085–6118; (*f*) F. Zeng and S. C. Zimmerman, *Chem. Rev.*, 1997, **97**, 1681–1712.

3 (*a*) I. G. Denisov, T. M. Makris, S. G. Sligar and I. Schlichting, *Chem. Rev.*, 2005, **105**, 2253–2278; (*b*) R. P. Cheng, S. H. Gellman and W. F. DeGrado, *Chem. Rev.*, 2001, **101**, 3219–3232; (*c*) P. G. Vasudev, S. Chatterjee, N. Shamala and P. Balaram, *Chem. Rev.*, 2011, **111**, 657–687; (*d*) S. L. Cravens, A. C. Navapanich, B. H. Geierstanger, D. C. Tahmassebi and T. J. Dwyer, *J. Am. Chem. Soc.*, 2010, **132**, 17588–17598.

4 (*a*) C. A. Hunter, K. R. Lawson, J. Perkins and C. J. Urch, *J. Chem. Soc., Perkin Trans. 2*, 2001, 651–669; (*b*) E. A. Meyer, R. K. Castellano and F. Diederich, *Angew. Chem., Int. Ed.*, 2003, **42**, 1210–1250; (*c*) F. G. Klarner and B. Kahlert, *Acc. Chem. Res.*, 2003, **36**, 919–932.

5 (*a*) L. Sobczyk, S. J. Grabowski and T. M. Krygowski, *Chem. Rev.*, 2005, **105**, 3513–3560; (*b*) M. Mautner, *Chem. Rev.*, 2005, **105**, 213–284; (*c*) M. Lamsa, J. Huuskonen, K. Rissanen and J. Pursiainen, *Chem.–Eur. J.*, 1998, **4**, 84–92.

6 (*a*) G. W. Gokel, W. M. Leevy and M. E. Weber, *Chem. Rev.*, 2004, **104**, 2723–2750; (*b*) M. M. Conn and J. Jr. Rebek, *Chem. Rev.*, 1997, **97**, 1647–1668; (*c*) L. M. Greig and D. Philip, *Chem. Soc. Rev.*, 2001, **30**, 287–302; (*d*) L. J. Prins, D. N. Reinhoudt and P. Timmerman, *Angew. Chem., Int. Ed.*, 2001, **40**, 2382–2426; (*e*) M. Kotera, J. M. Lehn and J. P. Vigneron, *J. Chem. Soc., Chem. Commun.*, 1994, 197; (*f*) R. P. Sijbesma and E. W. Meijer, *Curr. Opin. Colloid Interface Sci.*, 1999, **4**, 24; (*g*) G. A. Jeffrey, *An Introduction to Hydrogen Bonding*, Oxford University Press, New York, 1997; (*h*) J.-B. Guo, Y. Jiang and C.-F. Chen, *Org. Lett.*, 2010, **12**, 5764–5767; (*i*) J.-B. Guo, J.-F Xiang and C.-F. Chen, *Eur. J. Org. Chem.*, 2010, 5056; (*j*) J.-M. Zhao, Q.-S. Zong, T. Han, J.-F. Xiang and C.-F. Chen, *J. Org. Chem.*, 2008, **73**, 6800–6806.

7 (*a*) C. A. Hunter and J. K. M. Sanders, *J. Am. Chem. Soc.*, 1990, **112**, 5525–5534; (*b*) G. B. McGaughey, M. Gagne and A. K. Rappe, *J. Biol. Chem.*, 1998, **273**(25), 15458–15463; (*c*) C. G. Claessens and J. F. Stoddart, *J. Phys. Org. Chem.*, 1997, **10**, 254; (*d*) J. C. Nelson, J. G. Saven, J. S. Moore and P. G. Wolynes, *Science*, 1997, **277**, 1793; (*e*) C. A. Hunter, *Angew. Chem., Int. Ed. Engl.*, 1993, **32**, 1584–1586; (*f*) C. A. Hunter, *Chem. Soc. Rev.*, 1994, **23**, 101; (*g*) S. J. Cantrill, A. R. Pease and J. F. Stoddart, *J. Chem. Soc., Dalton Trans.*, 2000, 3715–3734; (*h*) A. D. Hamilton and D. V. Engen, *J. Am. Chem. Soc.*, 1987, **109**, 5035–5036; (*i*) M. Nishio and M. Hirota, *Tetrahedron*, 1989, **45**, 7201.

8 (*a*) V. F. Traven, *Frontier Orbitals and Properties of Organic Molecules*, Ellis Horwood, London, 1992, p. 67; (*b*) N. S. S. Kumar, M. D. Gujrati and J. N. Wilson, *Chem. Commun.*, 2010, **46**, 5464–5466; (*c*) S. I. Kato, T. Matsumoto, K. Ideta, T. Shimasaki, K. Goto and T. Shinmyozu, *J. Org. Chem.*, 2006, **45**, 3643–3647; (*d*) Q. Jiang, H. Y. Zhang, M. Han, Z. J. Ding and Y. Liu, *Org. Lett.*, 2010, **12**, 1728–1731.

9 (*a*) E. Barrett, T. J. Dale and J. J. Rebek, *J. Am. Chem. Soc.*, 2008, **130**, 2344–2350; (*b*) E. S. Barrett, T. J. Dale and J. J. Rebek, *Chem. Commun.*, 2007, 4224–4226; (*c*) E. Ishow, A. Credi, V. Balzani, F. Spadola and L. Mandolini, *Chem.–Eur. J.*, 1999, **5**, 984–989; (*d*) R. Ballardini, V. Balzani, A. Credi, M. T. Gandolfi and M. Venturi, *Acc. Chem. Res.*, 2001, **34**, 445–455 and references therein.

10 (*a*) M. Suresh, A. K. Mandal, M. K. Kesharwani, N. N. Adarsh, B. Ganguly, R. K. Kanaparthi, A. Samanta and A. Das, *J. Org. Chem.*, 2011, **76**, 138–144.

11 (*a*) A. J. Zych and B. L. Iverson, *J. Am. Chem. Soc.*, 2000, **122**, 8898–8909; (*b*) G. J. Gabriel, S. Sorey and B. L. Iverson, *J. Am. Chem. Soc.*, 2005, **127**, 2637–2640; (*c*) M. S. Cubberley and B. L. Iverson, *J. Am. Chem. Soc.*, 2001, **123**, 7560–7563.

12 (*a*) S. Kiviniemi, A. Sillanpaa, M. Nissinen, K. Rissanen, M. T. Lamsa and J. Pursiainen, *Chem. Commun.*, 1999, 897–898; (*b*) S. Kiviniemi, M. Nissinen, M. T. Lamsa, J. Jalonen, K. Rissanen and J. Pursiainen, *New J. Chem.*, 2000, **24**, 47–52; (*c*) M. Lee, Z. Niu, D. V. Schoonover, C. Slebodnick and H. W. Gibson, *Tetrahedron*, 2010, **66**, 7077–7082; (*d*) N. Noujeim, L. Leclercq and A. R. Schmitzer, *J. Org. Chem.*, 2008, **73**, 3784–3790.

13 (*a*) J. J. Reczek and B. L. Iverson, *Macromolecules*, 2006, **39**, 5601; (*b*) Z. M. Al-Badri and G. N. Tew, *Macromolecules*, 2008, **41**, 4173.

14 (*a*) C. P. Mandl and B. König, *J. Org. Chem.*, 2005, **70**, 670–674.

15 (*a*) M. Lamsa, J. Huuskonen, K. Rissanen and J. Pursiainen, *Chem.–Eur. J.*, 1998, **4**, 84–92; (*b*) M. Lamsa, T. Suorsa, J. Pursiainen, J. Huuskonen and K. Rissanen, *Chem. Commun.*, 1996, 1443–144; (*c*) M. Lamsa, J. Pursiainen, K. Rissanen and J. Huuskonen, *Acta Chem. Scand.*, 1998, **52**, 563.

16 (*a*) P. L. Gentili, F. Ortica and G. Favaro, *J. Phys. Chem. B*, 2008, **112**, 16793–16801; (*b*) P. P. H. Cheng, D. Silvester, G. Wang, G. Kalyuzhny, A. Douglas and R. W. Murray, *J. Phys. Chem. B*, 2006, **110**, 4637–4644.

17 A. C. Tedesco, D. M. Oliveira, Z. G. M. Lacava, R. B. Azevedo, E. C. D. Lima and P. C. Morais, *J. Magn. Magn. Mater.*, 2004, 2404–2405.

18 P. K. Behera, T. Mukherjee and A. K. Mishra, *J. Lumin.*, 1995, **65**, 131.